Arabian Journal of Geosciences (2020) 13: 632
https://doi.org/10.1007/s12517-020-05648-5

CAJG 2018 TOPIC 2

Application of remote sensing techniques in lithologic mapping of Djanet Region, Eastern Hoggar Shield, Algeria

Dalila Nemmour-Zekiri[1] · Fatiha Oulebsir[1]

Received: 30 August 2019 / Accepted: 30 June 2020 / Published online: 10 July 2020

Abstract
Application of remotely sensed data in geological mapping has been the subject matter of many studies in the last decades. The optimal exploitation of high spatial resolution satellite imagery can contribute to the improvement of the geological map, particularly when it comes to mapping in arid and desert areas where outcrops are often inaccessible. Djanet area lies in Eastern Hoggar Shield, Algeria. It is characterized by rather high corrugated reliefs and this makes it difficult to collect samples or even get field information from the entire region. The study covers the terrane of Djanet and part of the terrane of Edembo. In addition, this region is probably one of the least explored areas of Hoggar. This is why different remote sensing techniques have been used to make geologic mapping faster and more efficient. Processing of Landsat-7 ETM+ images covering the Djanet region includes various treatments ranging from contrast enhancements to spectral enhancements, and using images in 742 RGB color compositions, calculation processing of band ratios (3/1, 5/4, 7/5) and the (5/7, 2/1, 4/2) and the application of the directional filters, according to the orientations ranging from N000 up to N180E, with a semi-automatic approach for the extraction of lineaments to establish two maps, a lithological map and another linear map. The correlation of these maps with the field data allowed us to check the validity and the correspondence of the different facies and especially to clarify the lithological contours and the identification of the majority of the tectonic accidents derived from the analysis of Landsat satellite data. The geological map obtained gives another image of the region studied and provides new information on the contacts of the lithological units and the structural diagram.

Keywords Djanet area · Remote sensing technique · Eastern Hoggar

Introduction

The present work consists of a study of the Djanet area carried out essentially in the Neoproterozoic basement. This area is located at the northeast end of Eastern Hoggar (Fig. 1). It covers the terrane of Djanet and part of the terrane of Edembo (Black et al. 1994) (Fig. 1). The Djanet terrane is separated, to the west, from that of Edembo by the Ti n Amali shear zone (ZCTA) oriented NW-SE (Caby and Andreopoulos-Renaud 1987; Black et al. 1994). This area probably remains one of the least explored areas of Hoggar. It has only been the subject of a limited number of recent investigations (Bournas et al. 2003; Lamri et al. 2016; Fezaa et al. 2010, 2013; Oulebsir 2009; Zekiri-Nemmour 2012). However, the lack of a recent geological map led us to develop one in 2012 and it was this map that served as the basic document for our study.

The development of this detailed geological map was carried out thanks to the integration of remote sensing techniques and collected field data. The only use of conventional methods (field data and photo-interpretation analysis) for geological mapping remains insufficient, in particular due to the extent of the land, the abundant presence of wind deposits, and significant reliefs to which access in some areas is difficult or sometimes even impossible. On the other hand, high spectral and spatial resolution satellite imagery allowed us to identify

This paper was selected from the 1st Conference of the Arabian Journal of Geosciences (CAJG), Tunisia 2018

Responsible Editor: P. Anbazhagan

✉ Dalila Nemmour-Zekiri
dnemmour@usthb.dz; nemourd@yahoo.fr

Fatiha Oulebsir
foulebsir@yahoo.fr; fatiha.oulebsir@gmail.com

[1] University of Sciences and Technology Houari Boumediene (USTHB), El Alia Bab Ezzouar, .32 Algiers, BP, Algeria

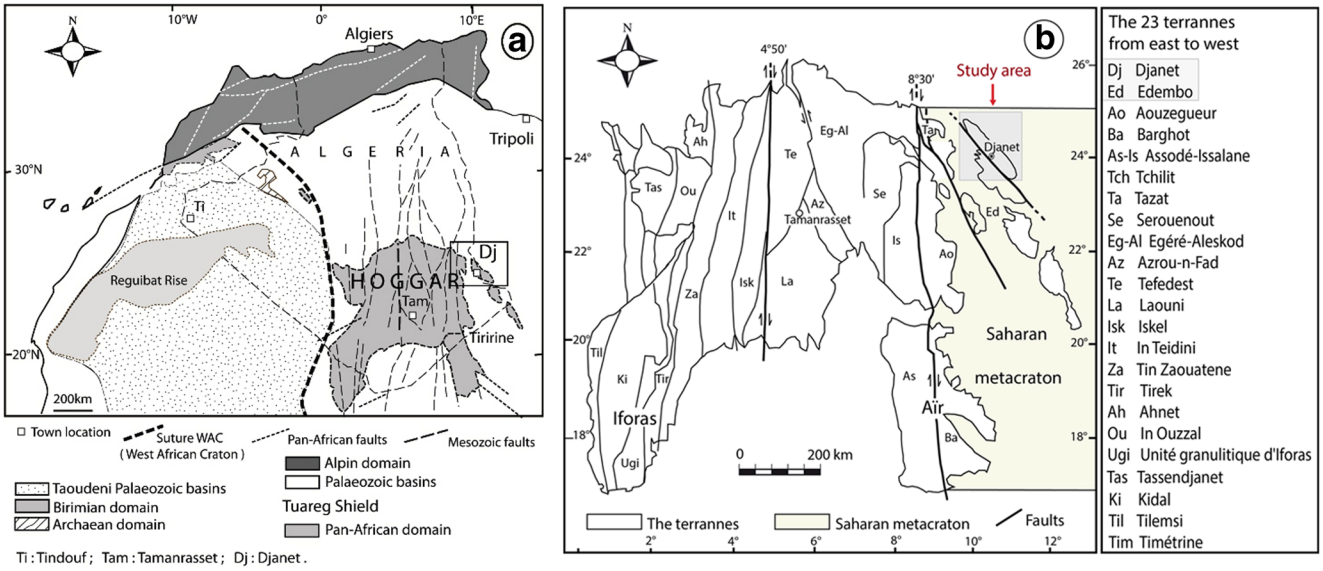

Fig. 1 Geologic maps (**a**) of Hoggar (Ennih and Liégeois 2001) and (**b**) of the study area (from the terrane map of the Touareg Shield (Black et al. 1994 et Liégeois et al. 2003))

even the different lithological units as well as the majority of tectonic accidents in order to improve the map and make it relatively more complete (Bonn and Rochon 1992; Bonn 1996; Caloz and Colet 2001; Chorowicz and Deroin 2004; Deroin 2019; Girard and Girard 1999; Sabins et al. 1987).

The study of lithological units and major accidents in the study area is essentially based on a semi-automatic approach, namely, the visual interpretation of digitally processed Landsat ETM+ multispectral images.

Geological setting

The Neoproterozoic basement of the Djanet area consists of two sets: (1) a granito-gneissic set outcropping to the west, in the Edembo terrane, and (2) an epizonal meta-sedimentary set of Neoproterozoic age called the series from Djanet. This series is intersected by magmatic rocks consisting essentially of granitoids and forms the terrane of Djanet. This set is surmounted to the north and east by the Cambro-Ordovician Paleozoic sandstones from Tassili n'Ajjer (Beuf et al. 1971) (Fig. 2). And finally, in our region of study, Cenozoic volcanism appears in the form of fairly well-preserved cones to the west in the ZCTA and to the north, in the Tassili sandstones (Fig. 3).

The granito-gneissic complex

The granito-gneissic complex appears in a rather discontinuous manner in the south and southwest of the study region and then disappears in the north under the Tassili sandstones. The oldest facies is represented by locally foliated migmatitic gneisses passing to ultramylonites. In places, these are intersected by other generations of porphyroid granites, the most common of which is a fine biotite granite, itself intruded by granites showing no internal deformation. The migmatization of the Ouhot area south of Ti n Amali, close to the shear zone (SZTA), was dated to 568 + 4 Ma, (Fezza et al. 2010).

In addition to this set, there is another type of porphyroid granite, slightly deformed. This granite is called Eferi granite; it is the most representative of the region. It contains dark or micaceous ovoid enclaves. The geochemical characteristics of these granites show a highly potent calcium-alkaline chemistry. In addition, the Eferi granite is intersected by veins (about 1 to 10 m) of pegmatites, aplite, and quartz, as well as numerous dykes, of plurimetric thickness, thus forming the vein complex of Ti n Amali. This vein network is represented by microgranites, microdiorites, and rhyolites. These are dated to 558 + 6 Ma (Fezza et al. 2010).

Fig. 2 Panoramic view of the different complexes in the Djanet region

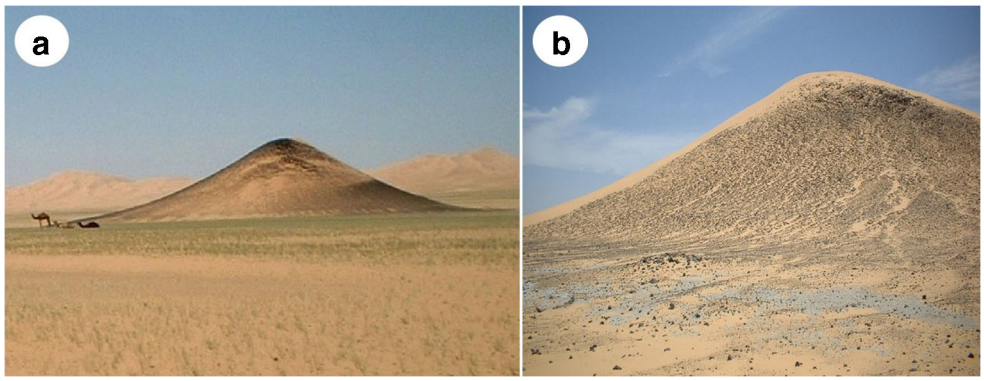

Fig. 3 Volcanism in the Djanet region

The sedimentary complex

The meta-sedimentary formations called "Djanet series" cover a large part of the Djanet region. This series is characterized by the predominance of schist and quartzite pelites. It is materialized by a rhythmic alternation (of sedimentary origin), micaceous beds, and quartz beds. In places, the facies become conglomerate, and even microconglomeric, characterized by pebbles of quartz rolled and stretched, in a micaceous detritic cement.

The flyschoid character of this series is attested, on the one hand, by the presence of slumps, grading, rhythmic repetition, oblique stratification, and containing pebbles clay, and on the other hand by the dominance of very thin deposits (Zekiri-Nemmour et al. 2006).

The meta-sedimentary formations are metamorphosed into the green shale facies. In addition, in contact with magmatic intrusions, the shale formations present a contact metamorphism, developing thin halos, corneal or spotted shales with andalusite. The sedimentation of this series takes place between 590 and 570 Ma (Fezaa et al. 2013).

Magmatism

The Djanet series is intersected by several late magmatic generations, forming granite massifs, of very varied shape and size. Due to only a partial geochronological dating of these massifs, we will classify them according to their shape and size.

Tissalatine granite

The Tissalatine granite has a teardrop shape, suggesting a placement along the Djanet fault, in a setting that is unstable on the east side. It is characterized by the presence of numerous dark microgranular enclaves. In the north of the massif, this granite with plagioclase phenocrysts is cut by pegmatites, by aplite, as well as by small basic masses of diorites. The geochemical characteristics of this granite show a calco-alkaline chemistry. In the northern part, this granite and its schistous host from the Djanet series are cut by gabbro veins in a global direction NW-SE to WNW-ESE. Currently, no dating has yet been carried out on this granite.

The granite of Djanet

Djanet's granite outcrops in the center of the city of Djanet, in the form of a large batholith. In the south, this granite shows intrusive contacts with the Djanet horizon series where it develops a very small halo of contact metamorphism, materialized by corneas and shales spotted with andalusite. All of these granites are furrowed with aplite and metric pegmatite. Finally, microgranite dykes pass through it. This porphyroid granite is dated to 571 + 16 Ma.

The granites of Gour Ti n Beguene, Tagment, Tassettouf and Tadjouisset

The granites of Gour Ti n Beguene, Tagment, Tassettouf, and Tadjouisset are characterized by a subcircular form masked in the east by the Tassili formations. Numerous microgranite veins of varying directions cross the massif. The geochemical characteristics of these granites show a high-potassium calco-alkaline chemistry. The installation of Gour Ti n Beguene granites (age 568 + 5 Ma) is believed to be contemporary with migmatization in the Edembo terrane (age 568 + 4 Ma).

The granites of Djeouet, Edjedje, Edjeriou, and Tin Ber

The granites of Djeouet, Edjedje, Edjeriou, and Tin Ber are in the form of small circular massifs of dimensions less than 2 km.

To the east of Tissalatine is the small massif of Edjedje, and to the southeast, the granite of Edjeriou, while the dome of Djeouet is located north of Djanet, and the pluton of Tin Ber in its center. The latter intersects Djanet's granite.

Only the Djeouet granite has been the subject of preliminary work (Oulebsir 2009). The Djeouet dome consists of various leucocratic granites, passing from a porphyroid facies in the center to a fine garnet granite at the periphery. The entire massif is cut by aplite and pegmatite veins as well as a few

microgranite veins. These granites are associated with specific mineralization (wolfram and cassiterite). The geochemical characteristics of these granites show an aluminous chemistry with a strong potassium calco-alkaline affinity. Consequently, the Djeouet granites correspond to the latest massifs in the region. They can be compared to the "Taourirt" granites, from the center and west of the Hoggar, which are set up at the end of the Pan-African orogeny, during the reactivation of large lithospheric faults (Boissonnas 1973; Azzouni-Sekkal et al. 2003).

The Ti n Amali vein complex

A very dense network of dykes and veins of porphyry rocks (microgranites, diorites, and rhyolites) intersects all the granites of Djanet, Eferi, and Gour Ti n Beguene. Rhyolites are compact rocks or fluid structures. In places, they contain enclaves of a millimeter order. In addition, we have observed a huge variation in facies between microgranites and microdiorites from one vein to another or sometimes even along the same vein. The geochemistry of these rocks shows that they belong to the strong potassium-based calco-alkaline series. Only the rhyolitic veins of the Ti n Amali region, oriented approximately NW-SE, have been dated. The ages obtained (558 + 6 Ma) seem to correspond to the last magmatic events in the region.

Materials and methods

The realization of this study required the use of a material composed of image data, topographic background, and data collected in the field as well as image processing software.

Data used

The images used for this study are satellite images of the Djanet region, acquired on November 29, 2000, by the ETM sensor from Landsat-7 and georeferenced in UTM-32-N, WGS 84. To cover the entire study area, we had to juxtapose the two scenes 190-043 (path 190, row 043) and 189-043 (path 189, row 043). These high-resolution images were chosen for their spectral and spatial characteristics allowing good lithological mapping.

The topographic map used corresponds to the sheet for Fort Charlet Djanet, NG-32-IV at 1/200,000, Clarke's ellipsoid, Universal Transverse Mercator (UTM) projection.

All the Landsat-7 ETM image processing works that led to the establishment of the litho-structural map and that of the detailed lineaments were performed using the ENVI 4.8 software, SIG MapInfo 8.0 and 10 and Adobe Illustrator CS6, while the statistical analysis of all the detectable lineaments from the directional filters was carried out with stereonet plotting program.

Methodology

The methodology adopted for this work is based on the processing of images of the study area, extracted from a mosaic of images. The focus is on the search for specific treatments allowing maximum lithological discrimination and good structural mapping. Indeed, two types of analyses were carried out on the image (Fig. 4).

The lithological discrimination was carried out on specific processing techniques, namely, the principal component analysis, the various colored compositions, and the RGB/HSV transformation produced from generated neo-bands. These techniques have made it possible to delimit the contours of all the formations thanks to the variation of the colors between two neighboring units.

On the other hand, the extraction of linear elements was carried out with a semi-automatic approach using digital processing based on the application of directional filters to multispectral images Landsat-7 ETM+ and on their visual interpretation (Scanvic 1983, 1992; Caloz and Collet 2001).

Image mosaic

When the extent of the study area exceeds the field of a remote sensing image, it becomes necessary to resort to the development of a mosaic of images. Indeed, these neighboring images have common areas between them, so that the merging makes it possible to obtain a single image which covers the entire scene based on the control of the main quality criteria (geometry and radiometry).

In the present work, the realization of a mosaic covering the whole of the region of Djanet was carried out

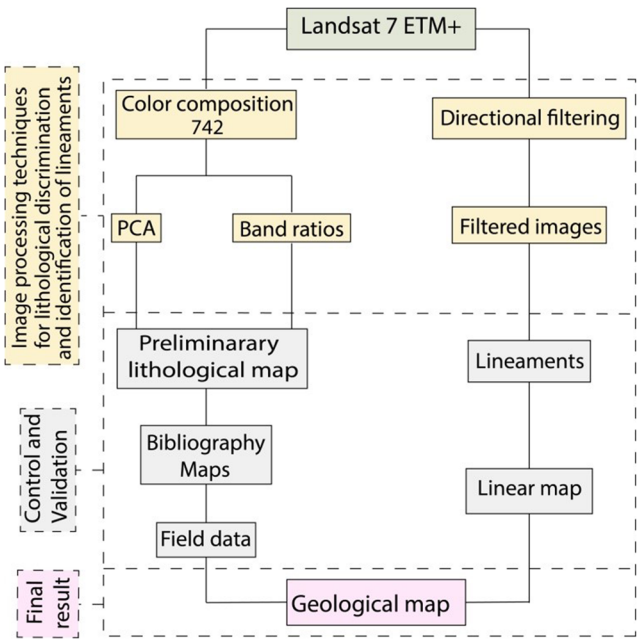

Fig. 4 Flowchart of the approach followed

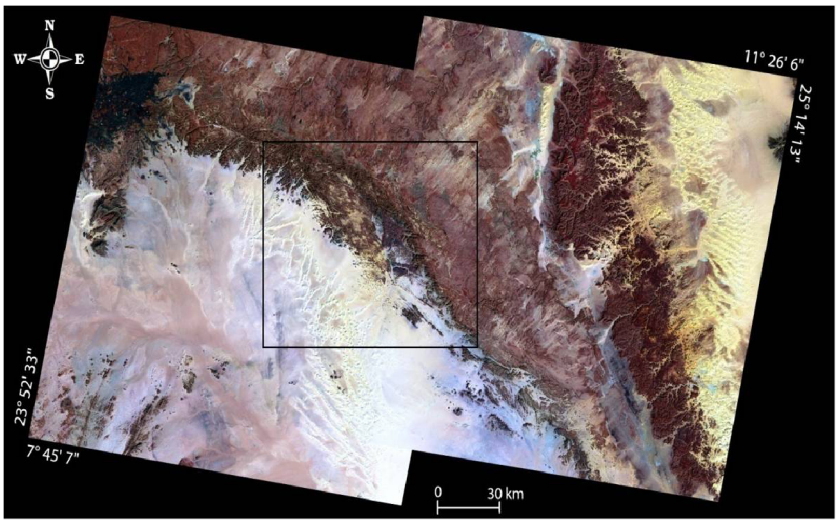

Fig. 5 Mosaic of the two scenes 190-043 and 189-043 ETM+ of Landsat in colored composition 742

by the partial superposition of two scenes 190-043 and 189-043 ETM+ of Landsat-7 (Fig. 5). As each scene corresponds to a fairly large region (185 × 185 km), we were led to make an extract for our study region.

Directional filters

Linear enhancement was carried out using directional filters in the four directions: N000°, N045°, N090°, and N135°. These filters were applied to band 7 with a square matrix of order 3, thus making it possible to better perceive the structural details (Bonn and Rochon 1992, Bonn 1996; Anudu et al. 2011, Caloz and Collet 2001; Scanvic 1992; Yao et al. 2012) (Fig. 6). The fracturing map obtained after the various treatments has approximately 3147 fractures of variable size and direction (Fig. 7A). The study of this map is based on the statistical analysis of all the detectable lineaments from the directional filters (Fig. 7B).

The results obtained show that all of the terrain in the region studied is affected by intense brittle deformation at different scales.

Color composition

The color composition of channels is 742 (combinations selected after carrying out a statistical study by calculating the correlation coefficient of the six bands, thus making it possible to reduce the information included in the 6 channels into only three RGB components; red, green, and blue are assigned to bands 7, 4, and 2, respectively). This combination is often used for geological applications.

Principal component analysis (PCA)

The analysis of selective main components PCA (PC1, PC2, PC3) made it possible to merge into a single image optimized to 90%, or even more, of the variance (information) contained in the original image files, thus providing a composition clear colored (Rakotoniaina 1998).

Band ratios

The analysis of the band reports made from the neo-bands generated makes it possible to produce new colored compositions.

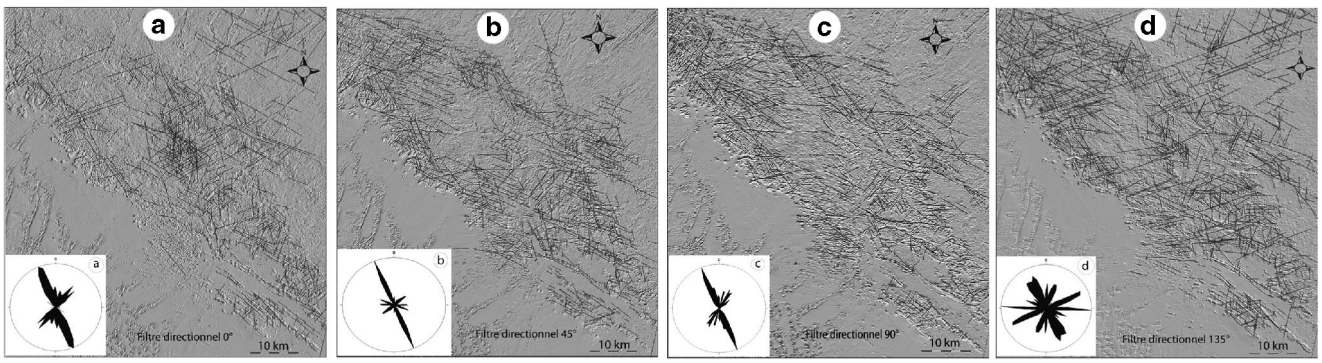

Fig. 6 (A, B, C, D) Fractures enhanced by filtered images with ETM+ 7. (a, b, c, d) Distribution diagrams of fractures' directions in the study area

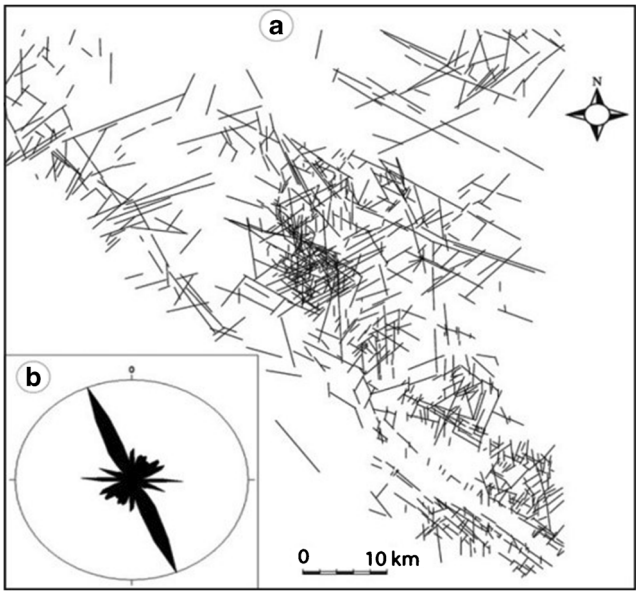

Fig. 7 (A) Detailed map of the fractures obtained from the filtered images. (B) Statistical characterization of the fracture populations

The compositions which have given us the best results in our region of study are 3/1, 5/4, 7/5 and 5/7, 2/1, 4/2.

Analysis and interpretation of results

Analysis of fracturing

From the synthesis of the lineaments extracted from the different images and after the various treatments, based on the enhancement and directional filtering of the Landsat-7 ETM+ image, it was possible to establish a linear map of the study area (Fig. 7). The study of this map shows that fracturing is organized according to four families of privileged directions (N-S, NW-SE, NE-SW, and E-W). The two main directions, NNW-SSE and NE-SW, were highlighted by the application of the two directional filters (000° and 090°) (Fig. 6 A and C), while the directions NW-SE and EW were determined from the directional filters 045° and 135° (Fig. 6 B and D).

The most important direction NNW-SSE to N-S corresponds to plurikilometric accidents which cross the region of Djanet from north to south. They affect both the Neoproterozoic terrain of the basement and their Paleozoic cover forming the Tassili sandstones. This direction is at the origin of shearing structures inducing a lenticular cutting compatible with dextral displacements. These N-S and NW-SE directions, identified both on satellite images and in the field, are confirmed by the interpretation of aeromagnetic data (Bournas et al. 2003).

On the other hand, the NE-SW direction corresponds to metric to kilometer faults which mainly affect the Paleozoic terrains. These are sinistral shears (Fig. 8).

Finally, the E-W direction corresponds to the kilometric faults that affect the entire region. These faults cut the structures they cross in several places, thus proving their recent nature. All of these directions have been identified both on satellite images and in the field.

Lithological discrimination

The objective of this study is to differentiate the varieties of rocks in the study area. In general, granites rich in quartz and feldspar have a lighter texture and a rough texture. Shales have a lighter tone and a smooth texture. On the other hand, the dykes and volcanic flows (essentially basalts), rich in magnesium and iron, have a darker tone and a rough texture. Sandstones rich in quartz showed a relatively clear tone.

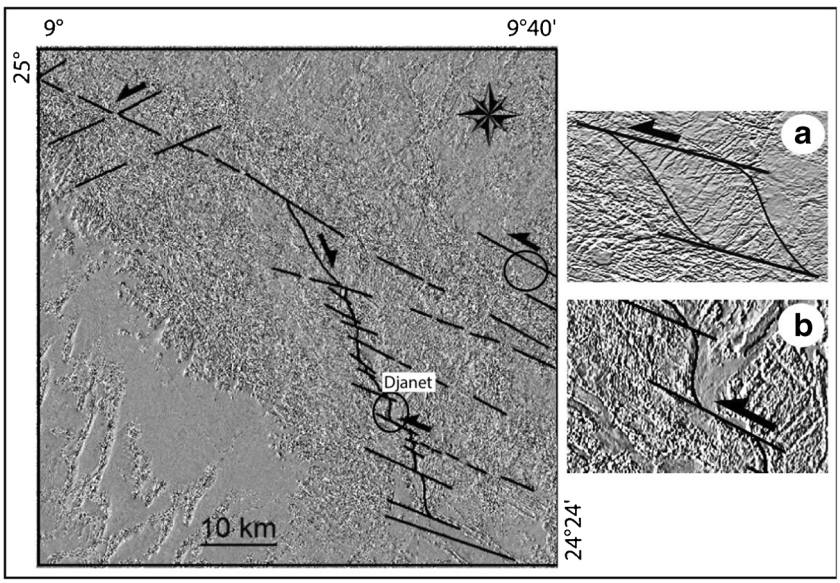

Fig. 8 Representation of the accident NNW-SSE from the directional filter. (a) NW direction indicates a sinistral shear; (b) NW-SE faults overlap the first and shift westward

	Bands ratios	Colors obtained	Rock name
a	ETM+3/ETM+1, ETM+5/ETM+4 et ETM+7/ETM+5	Purplish hue	Granites
		Orange	Djanet series
		Blue	Sandstones Tassili
		Dark brown	Diorite
		Purple	Gabbro
b	ETM +5/ETM+3, ETM+3/ETM+2, ETM +7/ETM+4	Blue	Gneiss
		Green	Djanet series
		Green	Sandstones Tassili
c	ETM+5/ETM+7, ETM+2/ETM+1 et ETM+4/ETM+2	Bluish	Rhyolite
		Purplish hue	Granites

Fig. 9 Summary table of a colored composition established from the different band ratios

The different colored compositions of the raw or transformed bands are used to bring out the homogeneous units in order to interpret the lithology of the Djanet region. All image processing has been done on small windows to clarify missing details on the map, especially in inaccessible areas.

Furthermore, from nine neo-bands coming from the band reports, (ETM + 3/ETM + 1, ETM + 5/ETM + 4, ETM + 7/ETM + 5, ETM + 5/ETM + 3, ETM + 3/ETM + 2, ETM + 7/ETM + 4, ETM + 5/ETM + 7, ETM + 2/ETM + 1, ETM + 4/ETM + 2), three RGB color compositions were produced. These colored compositions have the particularity of highlighting the different contours and make it possible to obtain an interesting maximum lithological discrimination thanks to the variation of the colors between two neighboring units (Fig. 9).

The application of the first treatment, north and south of the town of Djanet (Fig. 9a), brings out all the intrusive granite massifs of the Djanet series. This application makes it possible to specify, with a purplish hue, the outline of all the granites in the

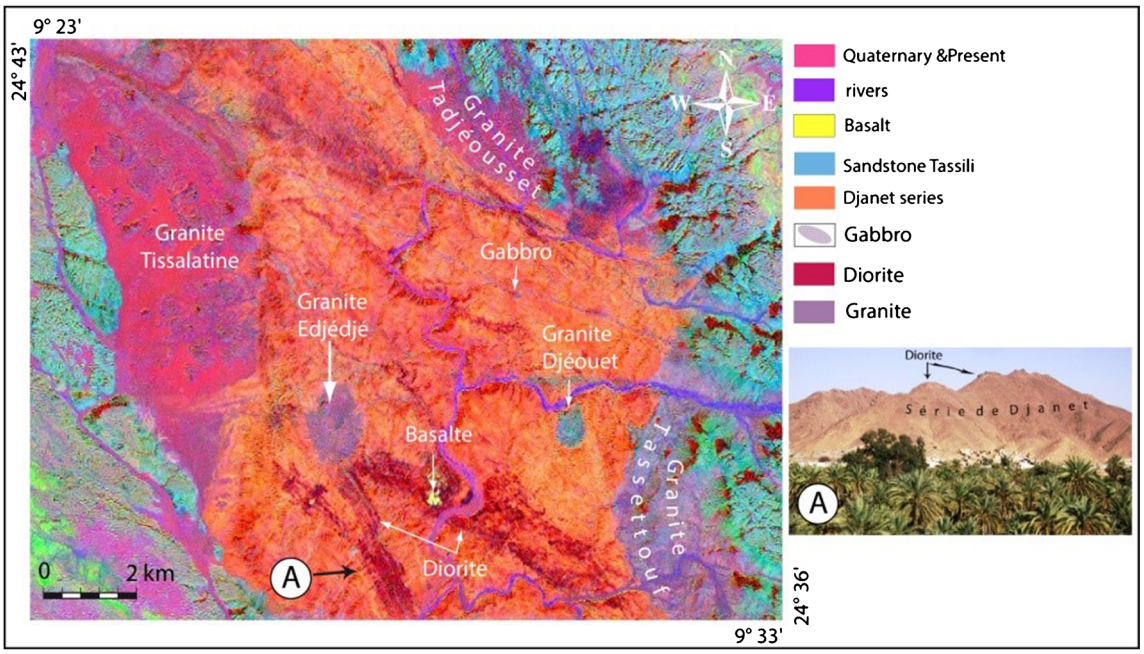

Fig. 10 Image of a colored composition established from the band ratios: ETM + 3/ETM + 1, ETM + 5/ETM + 4, and ETM + 7/ETM + 5. (A) Panoramic view of a diorite vein

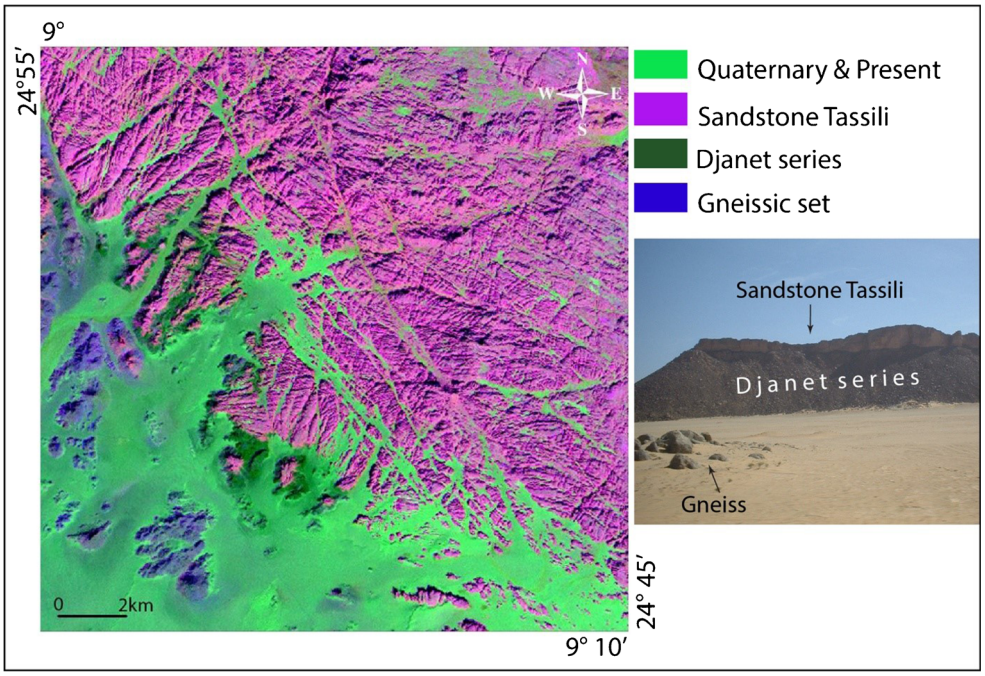

Fig. 11 Image of a colored composition established from the band ratios: ETM + 5/ETM + 3, ETM + 3/ETM + 2, and ETM + 7/ETM + 4

region. The formations of the Djanet series, tinted in orange, are distinct from the Paleozoic formations of Tassili n'Ajjer tinted in blue. The veins of diorite are strongly colored in dark brown, while the veins of gabbro appear in purple (Fig. 10).

The second treatment highlighted the other facies (Fig. 9b). The gneissic set appears in blue, the Djanet series in green, while the Tassili sandstones in purple (Fig. 11).

The third treatment (Fig. 9c) made it possible to identify homogeneous ranges comparable to dykes of bly-colored rhyolite and granites of a rather purplish hue (Fig. 12).

Contribution of remote sensing to mapping

The interpretation of all the satellite images resulted in the formation of a lithological map of the study area(Fig. 13). Comparison of this map with that given by conventional methods shows that all the main geological units of the region have been distinguished. The discrimination of these lithological units is based on the variation of the hues observed on the different image processing. Consequently, the different lithological units are well identified and appear under facies of distinct shades.

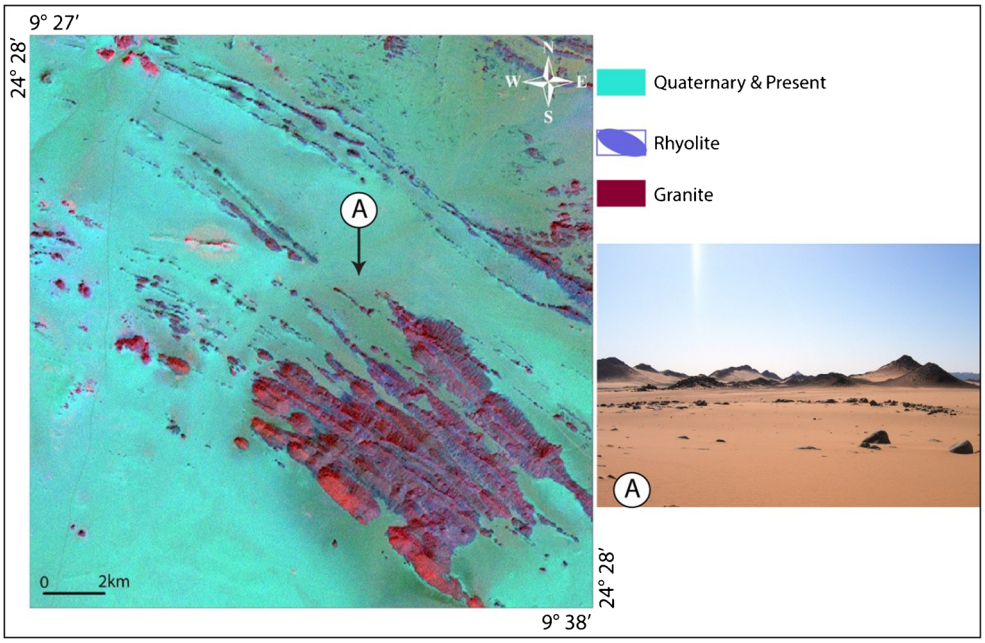

Fig. 12 Image of a colored composition established from the band ratios: ETM + 5/ETM + 7, ETM + 2/ETM + 1, and ETM + 4/ETM + 2

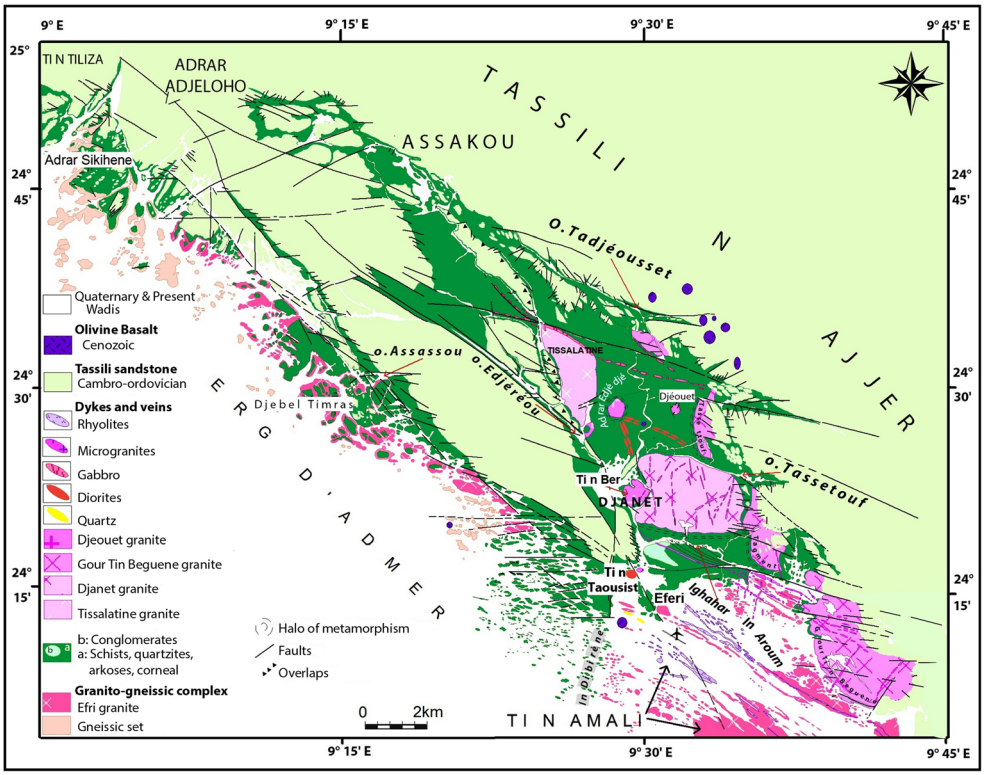

Fig. 13 Geological map based on field data and complemented by analysis of ETM+ Landsat images

The contours of the different granites in the study area are specified as well as the limits of the Djanet series. In addition, gabbro and diorite veins cut the shale formations of the Djanet series north and northeast of the city of Djanet. Although these veins are not mentioned on the previous geological map, these results are compatible with the field data.

The geological results obtained have been correlated with the various works already carried out in the region. The geological map thus obtained constitutes a detailed and fairly effective basic document (Fig. 10). It provides more information due to the new clarifications it brings.

Thus, we can see that the application of remote sensing in the geological field, essentially the analysis of litho-structural data, represents a very powerful complementary tool.

Conclusion

The present work is a contribution to the lithological and structural cartography from classical methods combined with the application of the remote sensing technique. The latter shows the contribution of satellite imagery to the mapping of geological contours, especially in inaccessible areas.

Indeed, the applied directional filters (N000°, N045°, N090°, N135°) made it possible to establish a linear mapping where more than 3140 lineaments of variable size and direction could be listed. Four families of preferred directions (N-S, NW-SE, NE-SW, and E-W) have been highlighted. These accidents played an important role in the structuring of the study region.

For the investigation of lithology in the region of study, the combination of all digital processing techniques, namely, spectral enhancement (742), principal component analysis, and the spectral band ratios ((3/1, 5/4, 7/5) and (5/7, 2/1, 4/2)), allowed an excellent distinction between the different lithological formations.

References

Anudu GK, Essien BI, Onuba LN, Ikpokonte AE (2011) Lineament analysis and interpretation for assessment of groundwater potential of Wamba and adjoining areas, Nasarawa State, Northcentral Nigeria. J Appl Technol Environ Sanit 1-2:185–198

Azzouni-Sekkal A, Liégeois JP, Bechiri-Benmerzoug F, Belaidi-Zinet S, Bonin B (2003) The "Taourirt" magmatic province, a marker of the very end of the Pan-African orogeny in the Tuareg Shield: review of the available data and Sr-Nd isotope evidence. J Afr Earth Sci 37: 331–350

Beuf S, Biju-Duval B, Charpal O, Rognon P, Gariel O, Bennacef A (1971). Les grès du paléozoïque inférieur au Sahara. Sédimentation et discontinuités. Évolution structurale d'un craton. Publ. Inst. Fr. Pétrole, Sci. et Tech. Du Pétrole n° 18, Edit. Technip, France

Black R, Latouche L, Liégeois JP, Caby R, Bertrand JM (1994) Pan-African displaced terranes in the Tuareg Shield (Central Sahara). Geology. 22:641–644

Bonn F (1996). Précis de télédétection. Vol. 2 : Applications thématiques. Presses de l'université du Québec/AUPELF, Sainte-Foy

Bonn F et Rochon G (1992). Précis de télédétection. Vol. 1 : Principes et Méthodes. Presses de l'université du Québec/AUPELF, Sainte-Foy

Bournas N, Galdeano A, Hamoudi M, Baker H (2003) Interpretation of the aeromagnetic map of Eastern Hoggar (Algeria) using the Euler deconvolution, analytic signal and local wavenumber methods. J Afr Earth Sci 37:191–205

Caby R, Andreopoulos-Renaud U (1987) Le Hoggar oriental, bloc cratonisé à 730 Ma dans la chaîne panafricaine du nord du continent africain. Precambrian Res 36:335–344

Caloz R, Collet C (2001) Précis de télédétection, vol 3: Traitements numériques d'images de télédétection. Presses de l'université du Québec, Québec

Chorowicz J, Deroin JP (2004) La télédétection et la cartographie géomorphologique et géologique. Éditions scientifiques GB (Contemporary Publishing International). Télédétection. 4-2:211–213

Deroin, JP (2019). An overview on 40 years of remote sensing geology based on Arab examples. Springer Geology: 427-453. https://doi.org/10.1007/978-3-319-96794-3

Ennih H, Liégeois JP (2001) The Moroccan anti-Atlas: the West African craton passive margin with limited Pan-African activity. Implications for the northern limit of the craton. Precambrian Res 112:289–302

Fezaa N, Liégeois JP, Nachida A, Cherfouh E, De Waelee B, Bruguierf O, Ouabadi A (2010) Late Ediacaran geological evolution (575–555 Ma) of the Djanet Terrane, Eastern Hoggar, Algeria, evidence for a Murzukian intracontinental episode. Precambrian Res 180:299–327

Fezaa N, Liégeois JP, Abdallah N, Bruguier O, Laouar R, Ouabadi A (2013) Origine du groupe métasédimentaire de Djanet (Hoggar oriental, Algérie). Géochronologie et géochimie Bulletin du Service Géologique National 24-1(1):24

Girard MC, Girard CM (1999) Traitement des données de télédétection. Dunod, Paris

Lamri T, Djemaï S, Hamoudi M, Zoheir B, Bendaoud A, Ouzegane K, Amara M (2016) Satellite imagery and airborne geophysics for geologic mapping of the Edembo area, Eastern Hoggar (Algerian Sahara). J Afr Earth Sci 115:143–158

Liégeois JP, Latouche L, Boughrara M, Navez J, Guiraud M (2003) The LATEA metacraton (Central Hoggar, Tuareg Shield, Algeria): behaviour of an old passive margin during the Pan-African orogeny. J Afr Earth Sci 37:161–190

Oulebsir F (2009) Pétrographie, géochimie et minéralisations à Sn-W associées du massif de Djilouet (Djanet, Hoggar Oriental). Thèse Magister, USTHB, Alger

Rakotoniaina S (1998) Analyse en composantes principales d'une image multispectrale de télédétection. Journal des Sciences de la Terre 2(3):5

Sabins JR, Freeman WH, Co SF (1987) Remote sensing: principles and interpretation. Geocarto International 2:251–251

Scanvic JY (1983) Utilisation de la télédétection dans les sciences de la terre. Manuels et Méthodes. BRGM, Orléans

Scanvic JY (1992) Télédétection aérospatiale et informations géologiques. Manuels et Méthodes. BRGM, Orléans

Yao TK, Fouché-Grobla O, Yéi Oga MS, Assoma VT (2012) Extraction de linéaments structuraux à partir d'images satellitaires, et estimation des biais induits, en milieu de socle précambrien métamorphisé. Revue Télédétection 10-4:161–178

Zekiri-Nemmour D (2012) Evolution thermo-mécanique et tectono-sédimentaire du bloc de Djanet (Hoggar oriental, Algérie). Thèse Doctorat d'Etat. USTHB, Alger

Zekiri-Nemmour D, Oulebsir F, Mahdjoub Y, Kesraoui M (2006) Eléments de géologie de la région de Djanet (Hoggar oriental, Algérie). The 3rd Conf Ass Afr Women Geoscie Maroc 166–167